

BCSJ Award Article

Conducting and Magnetic Properties of 1-Ethyl-3-methylimidazolium (EMI) Salts Containing Paramagnetic Irons: Liquids [EMI][$M^{III}Cl_4$] (M = Fe and $Fe_{0.5}Ga_{0.5}$) and Solid [EMI]$_2$[$Fe^{II}Cl_4$]

Yukihiro Yoshida,*[,1] Akihiro Otsuka,[1,2] Gunzi Saito,*[,1] Seiichi Natsume,[3] Eiji Nishibori,[3] Masaki Takata,[4] Makoto Sakata,[3] Masahide Takahashi,[5] and Toshinobu Yoko[5]

[1]Division of Chemistry, Graduate School of Science, Kyoto University, Sakyo-ku, Kyoto 606-8502

[2]Research Center for Low Temperature and Materials Sciences, Kyoto University, Sakyo-ku, Kyoto 606-8502

[3]Department of Applied Physics, Graduate School of Engineering, Nagoya University, Nagoya 464-8603

[4]Japan Synchrotron Radiation Research Institute (JASRI), 1-1-1 Kouto, Mikazuki-cho, Sayo-gun, Hyogo 679-5198

[5]Institute for Chemical Research, Kyoto University, Gokasho, Uji 611-0011

Received May 18, 2005; E-mail: yoshiday@kuchem.kyoto-u.ac.jp

An EMI-based room-temperature (RT) ionic liquid containing d^5 trivalent iron(III) ions [EMI][$Fe^{III}Cl_4$] was fully investigated, where EMI is 1-ethyl-3-methylimidazolium. The viscosity of the salt is 14 cP at 30 °C, and its ionic conductivity is as high as 1.8×10^{-2} S cm^{-1} at 20 °C. The high conductivity and fluidity can be attributed to the reduced interionic Coulomb attractions owing to the nephelauxetic effect. Magnetic susceptibility shows the Curie–Weiss behavior arising from $S = 5/2$ high-spin electronic state on iron(III) ions in both liquid and solid states, leading to the conductive–paramagnetic bifunctional RT ionic liquid. The solidified salt passes through an antiferromagnetic transition at 4.2 K. Diamagnetic [EMI][$Ga^{III}Cl_4$] and paramagnetic [EMI][$Fe^{III}Cl_4$]$_{0.5}$[$Ga^{III}Cl_4$]$_{0.5}$ are also RT ionic liquids and show similar conductivities (1.8–2.0 $\times 10^{-2}$ S cm^{-1} at 20 °C) and viscosities (12–13 cP at 30 °C). These results indicate that the influence of paramagnetic iron(III) ions upon the ionic conductivity and viscosity is negligible in the present system. A 2:1 EMI salt containing d^6 divalent iron(II) ions [EMI]$_2$[$Fe^{II}Cl_4$] melts at 86 °C. Its crystal structure determined by a synchrotron X-ray powder diffraction measurement is analogous to those of the reported [EMI]$_2$[$Co^{II}Cl_4$] and [EMI]$_2$[$Ni^{II}Cl_4$] with expanded lattice.

One of the main challenges in condensed matter science is the design of compounds exhibiting conductive and magnetic bifunctionality and the control of their competition and/or cooperation such as Kondo effect,[1] π–d interaction,[2] and giant magnetoresistance (GMR).[3] For liquid materials, some attractive properties and phenomena have been reported for inorganic liquids exhibiting both conductivity and magnetism, such as alkali and transition metals and alloys,[4] colloidal magnetic fluids dispersing iron nanoparticles,[5] and reversed Moses effect of copper sulfate aqueous solution.[6] In particular, magnetic fluids dispersing magnetic particles (e.g., magnetite and iron nitride) with a size of ca. 10 nm in diameter into water, kerosene, or various oils have been successfully applied in the engineering field to sealing, damping, and hydrodynamic bearings.[7] For organic systems, however, only a few dithiazolyl or dithiadiazolyl neutral radicals have been reported as paramagnetic liquids[8] which are unstable in air and are expected not to show an effective electric conductivity.

Ionic liquids (molten salts), especially those including 1,3-dialkylimidazolium (e.g., 1-ethyl-3-methylimidazolium, EMI, Scheme 1) cations, are promising materials for such a purpose because of their high ionic conductivities and low viscosities as well as high electrochemical and thermal stabilities (negligible vapor pressure).[9] It is thus possible that imidazolium-based ionic liquids containing anions with magnetic ions exhibit a thermal- and electrochemical-stable conductive-magnetic bifunctionality.[10] A brief report on the first well-charac-

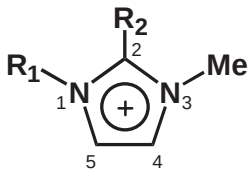

Scheme 1. Molecular structures of 1,3-dialkylimidazolium (EMI: $R_1 = Et$, $R_2 = H$; BMI: $R_1 = n$-Bu, $R_2 = H$; BDMI: $R_1 = n$-Bu, $R_2 = Me$).

Published on the web October 31, 2005; DOI 10.1246/bcsj.78.1921

terized conductive–paramagnetic bifunctional RT ionic liquid [EMI][$Fe^{III}Cl_4$] (**1**) containing d^5 trivalent iron(III) ions was recently presented by our group.[11] Here, we report the full studies on optical, electrochemical, transport, and magnetic properties of **1** in comparison with those of liquids containing diamagnetic gallium(III) ions [EMI][$Fe^{III}Cl_4$]$_{0.5}$[$Ga^{III}Cl_4$]$_{0.5}$ (**2**) and [EMI][$Ga^{III}Cl_4$] (**3**). Previous reports on [EMI]Cl/$Fe^{III}Cl_3$ and [EMI]Cl/$Ga^{III}Cl_3$ systems have been limited to cyclic voltammetry,[10a] and FAB-mass[12] and Raman spectroscopy,[13] respectively. Also a 2:1 EMI salt containing paramagnetic d^6 divalent iron(II) ions [EMI]$_2$[$Fe^{II}Cl_4$] (**4**) was prepared and its magnetic and structural properties were investigated.

Experimental

Materials. Anhydrous iron(II) chloride $FeCl_2$ (99.99%), iron(III) chloride $FeCl_3$ (99.99%), and gallium(III) chloride $GaCl_3$ (99.999%) were obtained from Aldrich and used without purification. [EMI]Cl was purchased from Tokyo Kasei (>97%) and purified according to the literature procedure.[14] Solvents (acetonitrile, ethyl acetate, and toluene) were distilled prior to use. All manipulations for the preparation of **1**–**4** were carried out under an inert atmosphere of helium gas in a glovebox with the rigid exclusion of air and moisture (H_2O, O_2 < 1 ppm).

Methods. UV–vis–NIR spectra were measured in acetonitrile (1500–200 nm) or in KBr pellet (2600–240 nm) on a Shimadzu UV-3100 spectrophotometer. FT-IR spectra were taken in KBr pellet with a Perkin-Elmer 1000 Series spectrophotometer (400–7800 cm^{-1}). Melting (T_m, onset of the endothermic peak), and decomposition (T_d) temperatures were determined by differential scanning calorimetry (DSC) thermograms (10 °C min^{-1} cooling/heating rate) on a Shimadzu DSC-60 instrument equipped with nitrogen cryostatic cooling, and the temperature was calibrated by water and indium. Density values were obtained by measuring the weight of the sample in a 1 cm^3 pycnometer held in the glovebox at 20 °C, that gave essentially the same density for [EMI]BF_4 (1.28 g cm^{-3}) as reported previously.[15] Viscosities were measured using a cone-type Tokyo Keiki rotational viscometer VISCONIC ED at 30 °C. Ionic conductivities were measured in a two platinum electrode conductivity cell (cell constant is 45 cm^{-1}, which was determined by 5×10^{-2}, 1×10^{-1}, and 5×10^{-1} M aqueous potassium chloride solutions), using an Agilent Technologies impedance analyzer 4294A over the frequency range from 40 Hz and 110 MHz (20–70 °C). The conductance of the samples was determined from the first real axis touchdown point in the Cole–Cole plot of the impedance data. For the electrochemical characterization, cyclic voltammetry measurements were performed using an ALS electrochemical analyzer 650A (22 °C). Working and counter electrodes were platinum, the reference electrode was Ag/AgCl, and the scan rate was 50 mV s^{-1}. A Quantum Design MPMS-XL SQUID magnetometer was used to collect DC magnetic susceptibility data between 1.9 and 400 K. The samples were sealed into quartz tubes of 5 mm diameter under ambient helium atmosphere. Data were corrected for molecular diamagnetism and holder contribution. High-resolution synchrotron X-ray powder diffraction measurements with an imaging plate as a detector were carried out on the beam line BL02B2 at SPring-8. The incident X-ray was monochromatized at a wavelength of 1.0 Å with a Si double crystal. The sample was sealed in a quartz capillary of 0.7 mm diameter under ambient helium atmosphere. The X-ray powder diffraction patterns was collected in 0.01° steps in 2θ from 4.0° to 40.0°, which corresponds to 1.43 Å resolution in *d*-spacing. The obtained data were analyzed by Rietveld refinement with bond lengths and bond angles restrained. Crystallographic data for **4** have been deposited with Cambridge Crystallographic Data Centre, CCDC No. 248622. Copies of the data can be obtained free of charge via http://www.ccdc.cam.ac.uk/conts/retrieving.html (or from the Cambridge Crystallographic Data Centre, 12, Union Road, Cambridge, CB2 1EZ, UK; Fax: +44 1223 336033; e-mail: deposit@ccdc.cam.ac.uk).

Syntheses and Characterization of [EMI][$M^{III}Cl_4$] (M = Fe (1), $Fe_{0.5}Ga_{0.5}$ (2), and Ga (3)). These RT ionic liquids were synthesized in a similar manner to that previously reported for [EMI][$Fe^{III}Cl_4$].[10a] Only the synthesis of **1** will be described here and other ionic liquids were obtainable similarly. Equimolar [EMI]Cl (3.00 g, 20.5 mmol) and $Fe^{III}Cl_3$ (3.32 g, 20.5 mmol) were mixed at RT without any solvent and the dark brown liquid **1** that formed was stirred for 2 days at RT. Salt **2** containing half-molar gallium(III) ions with d^{10} system is light brown, and salt **3** containing only gallium(III) ions is colorless. The characterizations were thoroughly carried out, since the contamination of the starting materials and/or water molecules substantially modify the intrinsic thermal and physical properties. Found: C, 23.35; H, 3.44; N, 9.17; Cl, 45.94%. Calcd for $C_6H_{11}Cl_4N_2Fe$: C, 23.34; H, 3.59; N, 9.07; Cl, 45.92%. IR (KBr) ν_{max}: 3161, 3148, 3118, 3103 (C–H aromatic), 2988, 2956 (C–H aliphatic), 1570, 1166 cm^{-1} (ring). UV–vis (acetonitrile) λ_{max} (ε): 685 (0.52), 616 (0.37), 530 (1.7), 361 (1.1×10^4), 312 (1.0×10^4), 241 (1.6×10^4) nm. ^{1}H NMR (400 MHz, D_2O) δ 1.44 (t, 3H, CH_3CH$_2$), 3.84 (s, 3H, CH_3), 4.16 (q, 2H, CH_3CH_2), 7.37 (s, 1H, CH), 7.44 (s, 1H, CH), 8.66 ppm (s, 1H, NCHN). For **2**: Found: C, 23.08; H, 3.39; N, 8.85; Cl, 45.03%. Calcd for $C_6H_{11}Cl_4N_2Fe_{0.5}Ga_{0.5}$: C, 22.82; H, 3.51; N, 8.87; Cl, 44.91%. IR (KBr) ν_{max}: 3163, 3150, 3121, 3102 (C–H aromatic), 2989, 2957 (C–H aliphatic), 1571, 1167 cm^{-1} (ring). UV–vis (acetonitrile) λ_{max} (ε): 685 (0.22), 617 (0.15), 531 (0.46), 362 (4.7×10^3), 312 (4.4×10^3), 241 (7.0×10^3), 211 (6.2×10^3) nm. ^{1}H NMR (400 MHz, D_2O) δ 1.42 (t, 3H, CH_3CH$_2$), 3.83 (s, 3H, CH_3), 4.15 (q, 2H, CH_3CH_2), 7.37 (s, 1H, CH), 7.44 (s, 1H, CH), 8.65 ppm (s, 1H, NCHN). For **3**: Found: C, 22.05; H, 3.28; N, 8.55; Cl, 43.94%. Calcd for $C_6H_{11}Cl_4N_2Ga$: C, 22.33; H, 3.44; N, 8.68; Cl, 43.95%. IR (KBr) ν_{max}: 3164, 3151, 3120, 3104 (C–H aromatic), 2990, 2958 (C–H aliphatic), 1571, 1167 cm^{-1} (ring). UV–vis (acetonitrile) λ_{max} (ε): 209 (4.6×10^3) nm. ^{1}H NMR (400 MHz, D_2O) δ 1.47 (t, 3H, CH_3CH$_2$), 3.86 (s, 3H, CH_3), 4.21 (q, 2H, CH_3CH_2), 7.39 (s, 1H, CH), 7.46 (s, 1H, CH), 8.68 ppm (s, 1H, NCHN).

Synthesis of [EMI]$_2$[$Fe^{II}Cl_4$] (4). A mixture of [EMI]Cl (1.01 g, 6.86 mmol) and $Fe^{II}Cl_2$ (0.436 g, 3.44 mmol) in acetonitrile (10 cm^3) was heated at reflux temperature for a day. After filtration, the pink solution was reduced to a half volume under reduced pressure. Addition of toluene (20 cm^3) affords a light pink solid that was recovered by filtration, washed with toluene (ca. 20 cm^3), and dried in vacuo (yield: 57%, 0.85 g). Found: C, 34.11; H, 5.33; N, 13.28; Cl, 33.73%. Calcd for $C_{12}H_{22}Cl_4N_4Fe$: C, 34.22; H, 5.28; N, 13.34; Cl, 33.77%. IR (KBr) ν_{max}: 3144, 3104, 3082 (C–H aromatic), 2991, 2953 (C–H aliphatic), 1574, 1172 cm^{-1} (ring). UV–vis (acetonitrile) λ_{max} (ε): 209 (2.5×10^4) nm. ^{1}H NMR (400 MHz, D_2O) δ 1.48 (t, 3H, CH_3CH$_2$), 3.87 (s, 3H, CH_3), 4.20 (q, 2H, CH_3CH_2), 7.40 (s, 1H, CH), 7.46 (s, 1H, CH), 8.68 ppm (s, 1H, NCHN). While the liquids **1**–**3** are fairly stable under atmospheric condition, the salt **4** is sensitive to aerobic oxidation, being instantly changed from pale pink solid to brown liquid (glass transition at −70 °C).

Table 1. Thermal and Physical Properties of **1**–**4**[a)]

Salt	T_m /°C	T_d /°C	d[b)] /g cm^{-3}	η[c)] /cP	σ[b)] /S cm^{-1}	χ[b)] /emu mol^{-1}
1	18	ca. 280	1.42[d)]	14	1.8×10^{-2}	1.4×10^{-2}
2	15	ca. 190	1.46[d)]	12	2.0×10^{-2}	7.8×10^{-3}
3	11	ca. 130	1.53[d)]	13	2.0×10^{-2}	0.0
4	86	ca. 270	1.419[e)]	—	—	1.1×10^{-2}

a) T_m = melting point, T_d = decomposition temperature, d = density, η = viscosity, σ = ionic conductivity, χ = magnetic susceptibility. b) At 20 °C. c) At 30 °C. d) By pycnometer. e) By structural refinement.

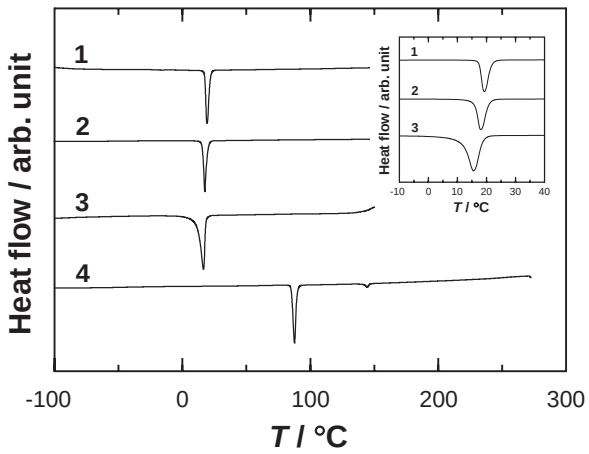

Fig. 1. DSC thermograms of **1**–**4** on heating process. The inset is the enlargement for the melting event range of **1**–**3**.

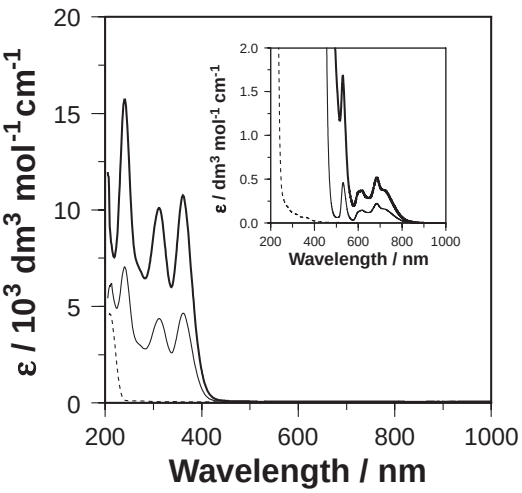

Fig. 2. Electronic absorption spectra of **1** (thick line), **2** (thin line), and **3** (dotted line) in acetonitrile. The inset is the enlargement for molar absorptivity in the visible range.

Results and Discussion

Thermal Properties. Thermal and physical properties of **1**–**4** are summarized in Table 1. Figure 1 presents DSC thermograms of **1**–**4**. The salts **1**–**3** are liquids at RT with the melting points within 11–18 °C. For the salt **2**, an additional endothermic peak at −23 °C disappears on heating at 150 °C for 5 min. Decomposition temperature of **1** is as high as 280 °C, leading to the wide liquid range (ca. 260 °C). An endothermic peak on melting of **2** is distinct from those of **1** and **3**, strongly indicating that the salt **2** is homogeneous instead of a heterogeneous mixture of **1** and **3**.

On cooling, a transformation from crystalline form to glass form passing through the supercooling liquid state was absent down to −100 °C for **1**–**4**. Similar behavior has been reported for [EMI]Cl/$AlCl_3$ system, in which the melt ranging in ratio [EMI]Cl/$AlCl_3$ from 0.64 to 1.27 shows no glass transition down to liquid nitrogen temperature.[16] A previous report has shown that the supercooled liquid [BMI][$Fe^{III}Cl_4$], where BMI is 1-*n*-butyl-3-methylimidazolium, passes through the glass transition at −85 °C,[10e] and recently we observed the glass transition of [BMI][$GaCl_4$] at −88 °C.[17] These results are indicative of the reduced reorientation energy for short alkyl chains of **1**–**3**, and could lead to the viscosities of **1**–**3** being lower than that of [BMI][$Fe^{III}Cl_4$] (vide infra).

The 2:1 salt **4** shows a melting event at 86 °C, which substantially exceeds the values of 1:1 salts **1**–**3**. The marked difference is readily explained in terms of the increased melting enthalpy that originates from the increased interionic Coulomb interactions, in a similar fashion to that from [BDMI][$Fe^{III}Cl_4$] (T_m < RT) to [BDMI]$_2$[$Fe^{II}Cl_4$] (T_m = 61 °C), where BDMI is 1-*n*-butyl-2,3-dimethylimidazolium.[10g] Also the temperature is lower than those of the isomorphous salts [EMI]$_2$[$Co^{II}Cl_4$] (T_m = 100–102 °C) and [EMI]$_2$[$Ni^{II}Cl_4$] (T_m = 92–93 °C),[18] and the variation of melting points might be related to the lattice volume (vide infra).

Optical Properties. Electronic absorption spectra are strongly indicative of high-spin electronic states for $Fe^{III}Cl_4$ anion in **1** and **2**, and $Fe^{II}Cl_4$ anions in **4**. Figure 2 shows absorption spectra of **1**–**3** in acetonitrile. Lowest-energy charge-transfer (CT) transitions $^6A_1 \rightarrow {}^6T_2$ of tetrahedral $Fe^{III}Cl_4$ anion in high-spin electronic state were observed centered at 361, 312, and 241 nm for **1** and **2**.[19] The very weak absorption bands observed in the range of 500–800 nm (Inset of Fig. 2) arise from d–d forbidden transitions: 685 nm ($^6A_1 \rightarrow {}^4T_1$), 616 nm ($^6A_1 \rightarrow {}^4T_2$), and 530 nm ($^6A_1 \rightarrow {}^4A_1$, ^4E).[19c,20] On the other hand, the salt **4** that contains iron(II) ions shows a d–d transition $^5E \rightarrow {}^5T_2$ in the near-infrared region,[19b,21] which is indicative of the rather low ligand field.

The infrared spectra of **1**–**3** are essentially identical. The two high frequency bands ranging of 3161–3164 and 3148–3151 cm^{-1} are assigned to the stretching mode of C(4)–H or C(5)–H bond of EMI cation, while the bands assigned to C(2)–H stretching mode appear at lower frequency regions

of 3118–3121 and 3102–3104 cm^{-1}. The corresponding aromatic C–H stretchings of **4** were observed at lower frequencies of 3144 and 3104 cm^{-1}, respectively. For **4**, an additional band centered at 3082 cm^{-1} is indicative of a significant level of C–H···Cl interionic interactions[18,22] as expected from its melting point being higher than those of **1**–**3**. The spectral features of **4** are essentially identical to those of the isomorphous $Co^{II}Cl_4$ and $Ni^{II}Cl_4$ salts.[18]

Electrochemical Window. The electrochemical stabilities of **1**–**3** were investigated at 22 °C. All ionic liquids are stable down to a low potential of around −2 V vs Ag/AgCl, below which the reductive decomposition of EMI cation occurs. A reversible wave for Fe(III)/Fe(II) redox process was observed for **1** and **2** at around 0.1 V as reported previously.[10a] In the oxidation scan, **1**–**3** were stable up to ca. +2 V regardless of the anion species, and it is thus apparent the salt **3** has a wide electrochemical window (ca. 4 V).

Ionic Conductivity and Viscosity. Ionic conductivities (σ) of **1**–**3** lie in the region of 1.8–2.0 × 10^{-2} S cm^{-1} at 20 °C. These values are comparable to those of 0.2 M KCl and 0.5 M $CuSO_4$ aqueous solutions, and those of the most conductive simple-type EMI salts [EMI][$AlCl_4$] (2.3 × 10^{-2} S cm^{-1} at 22 °C[16]), [EMI][$N(CN)_2$] (2.7 × 10^{-2} S cm^{-1} at 20 °C[23]), and [EMI][$C(CN)_3$] (1.8 × 10^{-2} S cm^{-1} at 20 °C[23]). However, the conductivities are apparently less than that of the double salt [EMI][$F(HF)_{2.3}$] (1.0 × 10^{-1} S cm^{-1} at 25 °C[24]), in which $F(HF)_2$ and $F(HF)_3$ anions are intermingled. Equivalent conductivities (Λ), which are represented by σ/M (M: molar concentration) for 1:1 electrolytes, are estimated to 3.9, 4.3, and 4.2 S cm^2 mol^{-1} at 20 °C for **1**–**3**, respectively. For [EMI][CF_3SO_3]/[EMI][$(CF_3SO_2)_2N$] binary system, the binary mixtures give a pronounced increase in Λ of 40–50% in comparison with those expected from a simple law of mixtures, which arises from the increase in charged carriers.[25] By contrast, the ionic conductivity of **2** involving equimolar $Fe^{III}Cl_4$ and $Ga^{III}Cl_4$ anions is comparable to those of the parent salts **1** and **3**, presumably due to the analogous anion species.

The viscosities (η) of **1**–**3** are also similar to each other (12–14 cP at 30 °C), and it is thus apparent that both the ionic conductivity and the viscosity of the present system do not depend on their magnetic properties. The viscosities are comparable to those observed for the most fluid simple-type EMI salts [EMI][$AlCl_4$] (18 cP at 25 °C[16]), [EMI][$N(CN)_2$] (17 cP at 22 °C[23]), and [EMI][$C(CN)_3$] (18 cP at 22 °C[23]), but still higher than the value for the double salt [EMI][$F(HF)_{2.3}$] (4.9 cP at 25 °C[24]).

Walden pointed out that the product of $\Lambda\eta$ remains constant over a wide range of aqueous solution systems.[26] The so-called Walden rule is interpreted in the same manner as the combination of the Nernst–Einstein equation $D_i = RT\Lambda_i/z_i^2F^2$ and the Stokes–Einstein equation $D_i = RT/6\pi N_A\eta r_i$ for the self-diffusivity (D_i) of species i with Λ_i in a medium with viscosity η, where z_i and r_i are the charge and radius of species i, and F and N_A are the Faraday constant and the Avogadro's number, respectively. It has recently become apparent that the rule applies well to ionic liquids formed with imidazolium analogue cations,[10e,23,27] and the present salts **1**–**3** also follow the relation on the basis of seventeen simple-type [EMI]X RT ionic liquids as seen in Fig. 3.[15,16,23,28] A deviation from the line obtained by least-squares fit would arise from the rather high measured temperature for viscosity (30 °C). The increased fluidity and conductivity of **1** in comparison with those of [BMI][$Fe^{III}Cl_4$] (ca. 30 cP and ca. 8 × 10^{-3} S cm^{-1} at 25 °C,[10e] and 31 cP and 8.9 × 10^{-3} S cm^{-1} at 25 °C[17]) as expected from the DSC thermograms are mainly caused by the shortened alkyl chain, which leads to the suppression of the vdW interactions between the chains. Similar trends of viscosity and conductivity for EMI and BMI salts have been reported for other anion systems, such as $F(HF)_{2.3}$,[27] $AlCl_4$,[16] BF_4,[15b] $C_nF_{2n+1}BF_3$ (n = 1, 2),[28d,e] and $(CF_3SO_2)_2N$.[28b]

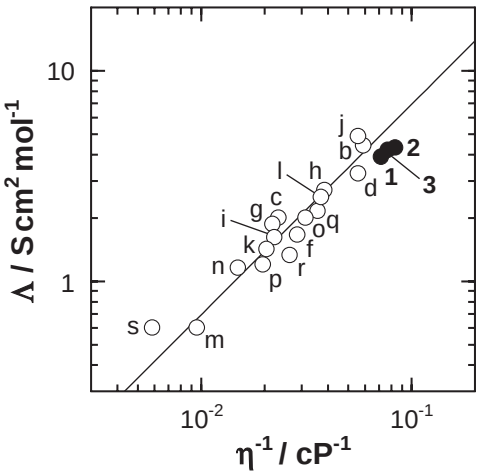

Fig. 3. A plot of the equivalent conductivity against the reciprocal of the viscosity for simple-type [EMI]X RT ionic liquids (X = (b) $N(CN)_2$,[23] (c) BF_4,[15,28a] (d) $C(CN)_3$,[23] (f) CF_3CO_2,[28b] (g) $CuCl_2$,[28c] (h) CF_3BF_3,[28d,e] (i) CF_3SO_3,[28b] (j) $AlCl_4$,[16] (k) NbF_6,[28f] (l) $C_2F_5BF_3$,[28e] (m) $C_3F_7CO_2$,[28b] (n) SbF_6,[28g] (o) $C_3F_7BF_3$,[28e] (p) TaF_6,[28f] (q) $(CF_3SO_2)_2N$,[28a,b] (r) $C_4F_9BF_3$,[28e] and (s) WF_7[28g]). A solid line is the least-squares fit to the data. The Λ values are unavailable for the (a) SCN[30a] and (e) SeCN[30b] salts due to the absence of density values.

Figure 4 shows the temperature dependence of ionic conductivity of **1**–**3** in the range of 20–70 °C. As temperature rises, the σ values increase according to the Arrhenius law $\sigma = \sigma_0\exp(-\mathcal{E}_a/k_BT)$, where the activation energy in conduction $\mathcal{E}_a$ was estimated to be 14.9, 14.5, and 14.8 kJ mol^{-1}, respectively. These values are significantly low in comparison with those of [EMI][BF_4] (17.6 kJ mol^{-1}), [EMI][$(CF_3SO_2)_2N$] (19.7 kJ mol^{-1}), and [EMI][$(C_2F_5SO_2)_2N$] (26.8 kJ mol^{-1}),[28a] and are comparable to that of the most conductive simple-type liquid [EMI][$N(CN)_2$] (15.2 kJ mol^{-1} [11b]). This indicates the rather low potential barrier for ionic conduction of **1**–**3**, in support of the high RT conductivities.

For organic syntheses, ionic liquids have been applied either as catalyst, as co-catalyst or catalyst activator, as source of new ligand for a catalytic metal center, or just as the solvent for the reaction.[29] The important property for such reactions is obviously to have low viscosity as well as the low vapor pressure, and the [BMI]Cl/$Fe^{III}Cl_3$ systems have been successfully applied for Friedel–Crafts acylation[10c] and carbonylation.[10d] Although the viscosity of **1**–**3** are apparently low in

comparison with that of [BMI][$Fe^{III}Cl_4$], they might be unfavorable as solvents for organic syntheses due to the melting point being near RT.

Relation between Conductivity and Molecular Weight. The high ionic conductivities of **1**–**3** are even more marked when the conductivity is plotted as a function of molecular weight of anion. The Λ value is represented by ionic conductivity (σ) and molar concentration (M) as $\Lambda = \sigma/M$, where M depending on ionic size, density, and molecular weight is closely related to the carrier concentration.[28b,e] Since the M value does not change widely in the EMI-based RT ionic liquids (3.9–6.5 $\times 10^{-3}$ mol cm^{-3}),[15,16,23,28] the ionic conductivity is a factor governing the equivalent conductivity. According to the Nernst–Einstein equation and the Einstein relation $D_i = \mu_i RT/|z_i|F$ for the relation between ion mobility (μ_i) and self-diffusivity of species i, the Λ value of the liquid composed of completely dissociated ions is normally proportional to the ion mobility, which is largely governed by the interionic interactions and molecular weight of ions. Figure 5 illustrates the plots of Λ and σ against the reciprocal of the molecular weight of anion (MW_a) for simple-type [EMI]X RT ionic liquids including the present three salts **1**–**3**.[15,16,23,28,30] Linear relations except for ionic liquids containing the tetrahedral anions with central metals, i.e., X = $AlCl_4$, $FeCl_4$ (**1**), $Fe_{0.5}Ga_{0.5}Cl_4$ (**2**), and $GaCl_4$ (**3**), strongly suggest that the MW_a is a factor governing the ionic conductivity in most EMI-based ionic liquids.[28b,e] It is then likely that the relatively high equivalent and ionic conductivities of **1**–**3** and the $AlCl_4$ salt in comparison with those expected from the linear relation are mainly caused by the reduced interionic interactions. Previously, the Xα calculations predicted the charge distribution in $FeCl_4^-$ anion to be +0.916 for Fe and −0.479 for Cl as the covalency in M–Cl (M = Al, Ga, or Fe) bonds increases due to the nephelauxetic effect.[31] It thus appears that this effect is associated with the highly ionic conductivities observed for **1**–**3** and the $AlCl_4$ salt, owing to the reduced interionic Coulomb attractions. The nephelauxetic series has been established in the order of covalency in the metal–ligand bond: $F^- < H_2O < NH_3 <$ 1,2-ethanediamine $< SCN^- < Cl^- < CN^- < Br^-$.[32] To account for a contribution of molecular weight to the conductivity, tetracyanometallate monoanions of trivalent metals $[M^{III}(CN)_4]^-$ would be promising for highly conductive ionic liquids although the significant coordination ability of cyano groups. The ionic conductivity of the SCN salt is extraordinary low (ca. 8 $\times 10^{-3}$ S cm^{-1} at 25 °C[30a]) in comparison with that expected from the linear relation in Fig. 5b, although its viscosity (21 cP) is as low as that of the highly conductive $N(CN)_2$ salt with comparable MW_a. The peculiar feature is indicative of the reduced carriers in the liquid, which might be caused by the ion association or ion pairing of a significant fraction of oppositely charged ions and/or the formation of neutral thiocyanogen $(SCN)_2$.

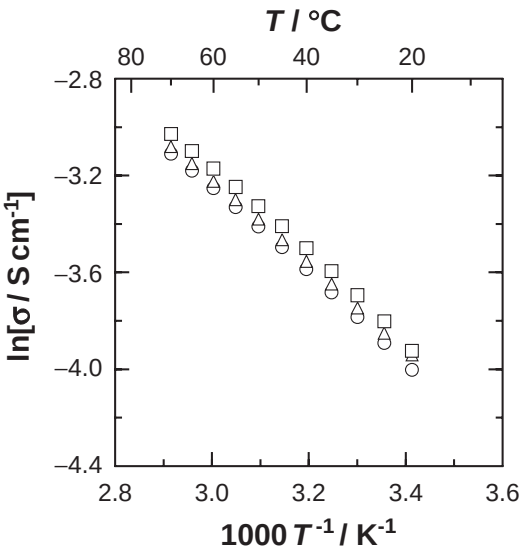

Fig. 4. Temperature dependence of ionic conductivity of **1** (○), **2** (△), and **3** (□).

Magnetic Properties. Ionic liquids **1** and **2** containing iron(III) ions exhibit a paramagnetic behavior at around RT,

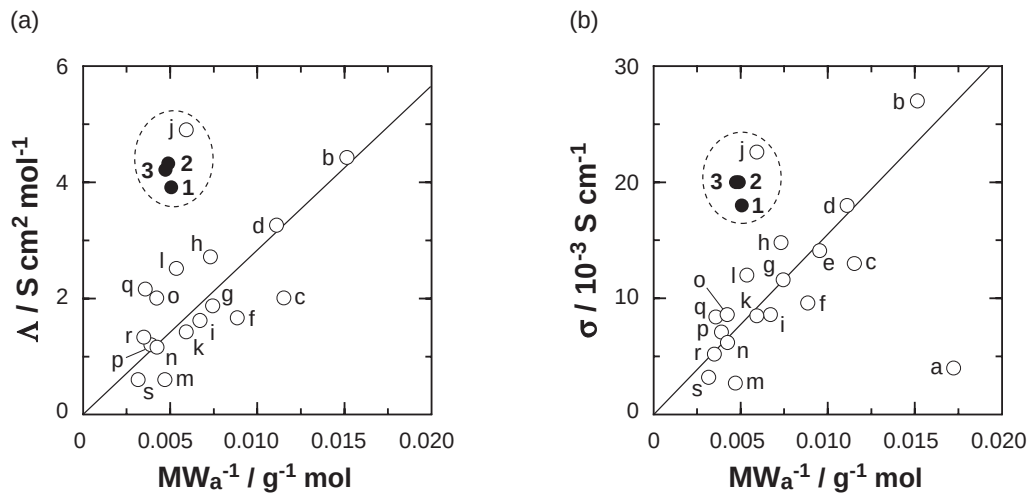

Fig. 5. A plots of (a) equivalent conductivity and (b) ionic conductivity against the reciprocal of the molecular weight (MW_a) of anion for simple-type [EMI]X RT ionic liquids. Indices are identical with those in Fig. 3.[15,16,23,28,30] Solid lines act as a guide to viewing.

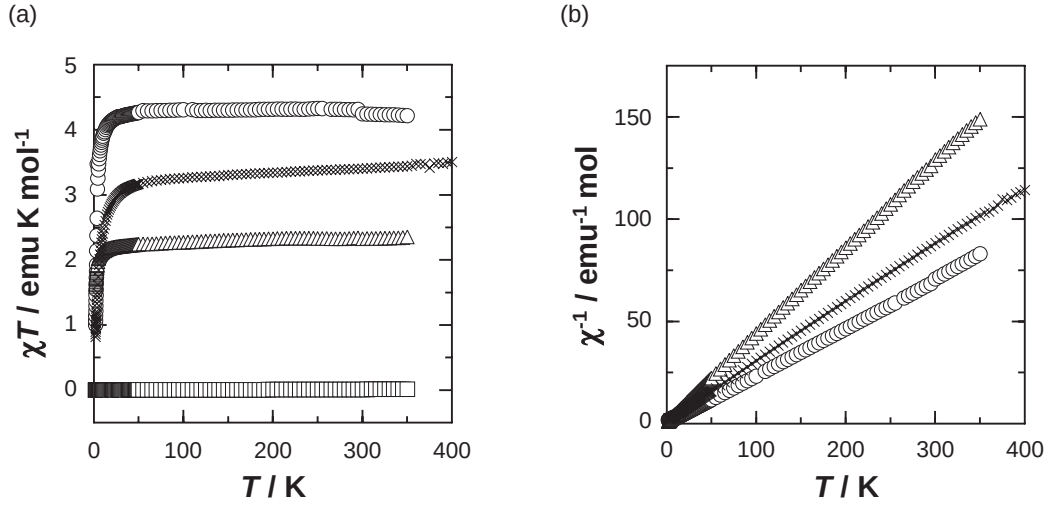

Fig. 6. Temperature dependence of (a) χT and (b) χ^{-1} of **1** (○), **2** (△), **3** (□), and **4** (×) in an applied field of 100 Oe on heating process.

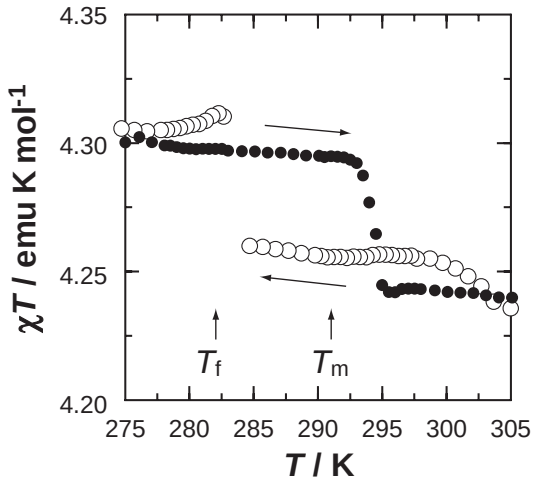

Fig. 7. Temperature dependence of χT of **1** in the temperature range of 275–305 K on heating (●) and cooling (○) processes in an applied field of 10 kOe.

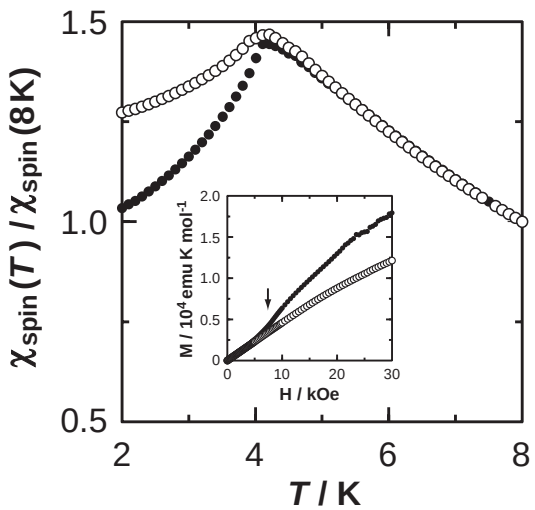

Fig. 8. Temperature dependence of static susceptibility of **1** below 8 K. Data are collected after cooling down to 4 K from 300 K by slow cooling (-0.5 K min^{-1}, ●) and by quenching (○). Inset is the field dependence of magnetization at 2 K (●) and 8 K (○).

and the effective magnetic moments (μ_{eff}) were found to be $5.83\mu_{\text{B}}$ and $4.31\mu_{\text{B}}$ at 300 K (both are in liquid state), respectively. It is thus apparent that **1** and **2** are bifunctional liquids with high ionic conductivities and paramagnetic behaviors.[11] The estimated μ_{eff} values are significantly large in comparison with the dithiazolyl or dithiadiazolyl neutral radicals (ca. $1.3\mu_{\text{B}}$),[8,33] and are unambiguously originated from the $Fe^{III}Cl_4$ anions with $S = 5/2$ high-spin electronic state (spin-only values are $5.92\mu_{\text{B}}$ and $4.18\mu_{\text{B}}$, respectively). The salt **3** containing only gallium(III) ions are diamagnetic. Figure 6a shows the product of static susceptibility (χ) and temperature for **1**–**4** as a function of temperature. On cooling, the χT value of **1** shows an abrupt jump of 5×10^{-2} emu K mol^{-1} at 284 K (Fig. 7), which is close to the freezing point of 282 K. Although we do not have information about the low-temperature crystal structure and optical properties at present, it is unambiguously evident that a solidification of **1** is related to the upturn since the χT value during the heating process falls by a similar amount 5×10^{-2} emu K mol^{-1} at 293–295 K near the melting point (291 K). This observation is contrary to our simple expectation that the solid phase has significant antiferromagnetic interactions between $Fe^{III}Cl_4$ anions in comparison with those in liquid phase. The thermal hysteresis is independent of the magnetic field up to 50 kOe. Below 270 K, the χT values of **1** and **2** remain almost constant down to 30 K, where it then begins to fall owing to the antiferromagnetic interactions between iron(III) ions. Temperature dependence of the both salts down to 10 K follows the Curie–Weiss expression with $\chi = C(T - \theta)^{-1}$ (Fig. 6b), where the Curie constant (C) and the Weiss temperature (θ) are estimated to be 4.33 emu K mol^{-1} and -0.9 K for **1**, and 2.34 emu K mol^{-1} and -1.7 K for **2**. On further cooling, however, **1** and **2** behave quite differently. The salt **1** exhibits a susceptibility kink at 4.2 K, below which it loses a significant fraction of its susceptibility (Fig. 8). Both the absence of hysteresis between zero

field cooling (ZFC) and field cooling (FC) processes and the observation of spin-flop at ca. 8 kOe (inset of Fig. 8) strongly indicate that the behavior is not due to the spin-glass forming, but arises from the long-range antiferromagnetic ordering. Magnetic behaviors below the transition depend on the cooling rate. The slowly cooled ($-0.5\,\mathrm{K\,min^{-1}}$) sample shows a gradual decrease in susceptibility of ca. 30%, which is usual for non-oriented antiferromagnets. For the quenched sample, the loss of susceptibility is rather small due to either insufficient crystallinity to form the long-range magnetic ordering or formation of paramagnetic and antiferromagnetic domains. For the salt **2**, on the other hand, the temperature dependence follows the Curie–Weiss law down to 1.9 K, possibly owing to the magnetic dilution by diamagnetic $Ga^{III}Cl_4$ anions. This finding again indicates that the solidified salt **2** is homogeneous instead of a heterogeneous mixture of **1** and **3**.

The salt **4** also obeys the Curie–Weiss expression with $C = 3.481\,\mathrm{emu\,K\,mol^{-1}}$ and $\theta = -5.6$ K regardless of its forms, i.e., liquid or solid. The effective moment of $5.22\mu_B$ substantially exceeds the value expected for paramagnetic $S = 2$ spin system (spin-only value is $4.90\mu_B$). This is found to be the case in most of the $Fe^{II}Cl_4$ salts ($5.3–5.4\mu_B$),[19b,21a,c,34] and results from the total effects of the mixing-in of the first excited state into the ground state via spin-orbit coupling, temperature-independent paramagnetism, and some thermal contribution from the $3d^5 4s$ configuration.[34]

Crystal Structure of 4. Since attempts to obtain the single crystals suitable for single-crystal X-ray diffraction studies were unsuccessful, high-resolution synchrotron X-ray powder diffraction measurements were carried out for polycrystals **4** at 300 K and the diffraction profiles were analyzed by the Rietveld method. The peak positions and intensities of Bragg reflections were similar to those of the reported $[EMI]_2[Co^{II}Cl_4]$ and $[EMI]_2[Ni^{II}Cl_4]$ salts,[18] and thus the structure parameters of the $Co^{II}Cl_4$ salt were used as the starting model for the refinement. The salt **4** belongs to the tetragonal system: space group $I4_1/a$, $a = 14.14626(4)$, $c = 19.63368(9)$ Å, $V = 3929.03(4)\,\mathrm{Å^3}$, $Z = 8$, $D_{calcd} = 1.419\,\mathrm{g\,cm^{-3}}$, $R_I = 0.039$, $R_{wp} = 0.023$, and is isostructural to those of the reported $[EMI]_2[Co^{II}Cl_4]$ and $[EMI]_2[Ni^{II}Cl_4]$ salts as expected.[18] The unit cell is apparently expanded compared with those of the $Co^{II}Cl_4$ ($3890(1)\,\mathrm{Å^3}$) and $Ni^{II}Cl_4$ ($3871(2)\,\mathrm{Å^3}$) salts. The low melting point of **4** (86 °C) in comparison with those of the two isomorphous salts (100–102 °C for $Co^{II}Cl_4$, 92–93 °C for $Ni^{II}Cl_4$) is largely related to the expanded lattice, which gives rise to the reduced melting enthalpy.

The crystal contains one crystallographically independent EMI cation and two $FeCl_4$ anions ($Fe(1)Cl(1)_4$ and $Fe(2)Cl(2)_4$). Four EMI cations surround the anionic unit with Fe(2) in a tetrahedral fashion involving hydrogens bonded to C(2) positions (Fig. 9a). On the other hand, the anion with Fe(1) is surrounded tetrahedrally by eight EMI cations, where each Cl(1) is connected with two distinct EMI cations through C(4)–H···Cl(1) and C(5)–H···Cl(1) hydrogen bonding type interactions. Accordingly, the EMI cation is surrounded by three anions as seen in Fig. 9b. The shortest C(2)–H···Cl(2), C(4)–H···Cl(1), and C(5)–H···Cl(1) distances are found to be 3.261(4), 3.617(9), and 3.526(9) Å, respectively, which are much less than the sum of the vdW radii (3.95 Å).[35] These hydrogen bonds are reminiscent to those observed in the $Co^{II}Cl_4$ and $Ni^{II}Cl_4$ salts, and are consistent with the infrared absorption band arising from C–H···Cl interionic interactions. No short cation···cation contacts were found in the three isostructural tetrachlorometallate salts.

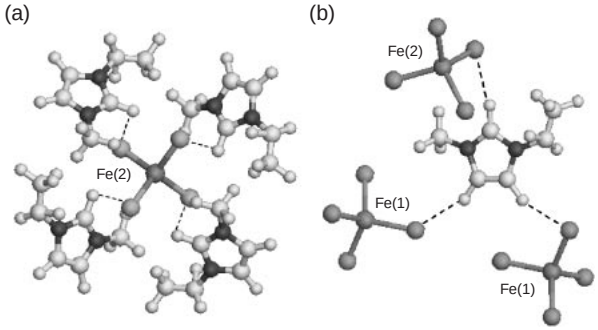

Fig. 9. Interionic contacts between EMI cation and $Fe^{II}Cl_4$ anion in the polycrystalline **4** (a) around Fe(2) ion and (b) around EMI cation at 300 K. Short C–H···Cl contacts are shown by dashed lines.

Conclusion

We obtained conductive–paramagnetic bifunctional RT ionic liquids $[EMI][Fe^{III}Cl_4]$ showing $\sigma = 1.8 \times 10^{-2}\,\mathrm{S\,cm^{-1}}$ and $\chi = 1.4 \times 10^{-2}\,\mathrm{emu\,mol^{-1}}$ at RT and $[EMI][Fe^{III}Cl_4]_{0.5}$-$[Ga^{III}Cl_4]_{0.5}$ showing $\sigma = 2.0 \times 10^{-2}\,\mathrm{S\,cm^{-1}}$ and $\chi = 0.8 \times 10^{-2}\,\mathrm{emu\,mol^{-1}}$ at RT. On cooling $[EMI][Fe^{III}Cl_4]$ passes through an antiferromagnetic transition at 4.2 K, while $[EMI][Fe^{III}Cl_4]_{0.5}[Ga^{III}Cl_4]_{0.5}$ follows the Curie–Weiss law down to 1.9 K. The colorless liquid $[EMI][Ga^{III}Cl_4]$ is diamagnetic, but its ionic conductivity ($2.0 \times 10^{-2}\,\mathrm{S\,cm^{-1}}$ at 20 °C) is comparable to those of $[EMI][Fe^{III}Cl_4]$ and $[EMI]$-$[Fe^{III}Cl_4]_{0.5}[Ga^{III}Cl_4]_{0.5}$. These findings strongly suggest that the influence of paramagnetic iron(III) ions upon the ionic conductivity is negligible in the present system. Possible nephelauxetic effect in halogenometallate anions would be promising for future exploration of the highly conductive ionic liquids, as well as the paramagnetic liquids with sizable magnetic moment. The crystal structure of $[EMI]_2[Fe^{II}Cl_4]$ was determined by synchrotron X-ray powder diffraction measurements. It appears that its lower melting point than those of isomorphous $Co^{II}Cl_4$ and $Ni^{II}Cl_4$ salts is related to its expanded lattice.

This work was in part supported by a COE Research on Elements Science (No. 12CE2005) and a Grant-in-Aid (21st Century COE programs on Kyoto University Alliance for Chemistry and on Nagoya University Alliance of Frontiers of Computational Science) from the Ministry of Education, Culture, Sports, Science and Technology, Japan. The authors also acknowledge the financial support from the Grants-in-Aid for Scientific Research (No. 15205019) by JSPS.

References

1 a) J. Kondo, *Prog. Theor. Phys.*, **32**, 37 (1964). b) H. Tsunetsugu, M. Sigrist, and K. Uedo, *Rev. Mod. Phys.*, **69**, 809 (1997).

2 a) K. Yamaguchi, Y. Kitagawa, T. Onishi, H. Isobe, T. Kawakami, H. Nagao, and S. Takamizawa, *Coord. Chem. Rev.*, **226**, 235 (2002). b) T. Enoki and A. Miyazaki, *Chem. Rev.*, **104**, 5449 (2004).

3 a) M. N. Baibich, J. M. Broto, A. Fert, F. Nguyen Van Dau, and F. Petroff, *Phys. Rev. Lett.*, **61**, 2472 (1988). b) B. Dieny, V. S. Speriosu, S. S. P. Parkin, B. A. Gurney, D. R. Wilhoit, and D. Mauri, *Phys. Rev. B*, **43**, 1297 (1991). c) D. E. Heim, R. E. Fontana, C. Tsang, V. S. Speriosu, B. A. Gurney, M. L. Williams, A. Friederich, and J. Chazelas, *IEEE Trans. Magn.*, **30**, 316 (1994). d) E. Y. Tsymbal and D. G. Pettifor, *Solid State Phys.*, **56**, 113 (2001).

4 a) N. H. March, *Can. J. Chem.*, **55**, 2165 (1977). b) F. Hensel, *Angew. Chem., Int. Ed. Engl.*, **19**, 593 (1980), and references therein.

5 S. Odenbach, *J. Phys.: Condens. Matter*, **16**, R1135 (2004).

6 N. Hirota, T. Homma, H. Sugawara, K. Kitazawa, M. Iwasaka, S. Ueno, H. Yokoi, Y. Kakudate, S. Fujiwara, and M. Kawamura, *Jpn. J. Appl. Phys.*, **34**, L991 (1995).

7 K. Raj and R. Moskowitz, *J. Magn. Magn. Mater.*, **85**, 233 (1990).

8 a) E. G. Awere, N. Burford, C. Mailer, J. Passmore, M. J. Schriver, P. S. White, A. J. Banister, H. Oberhammer, and L. H. Sutcliffe, *J. Chem. Soc., Chem. Commun.*, **1987**, 66. b) W. V. F. Brooks, N. Burford, J. Passmore, M. J. Schriver, and L. H. Sutcliffe, *J. Chem. Soc., Chem. Commun.*, **1987**, 69. c) S. Brownridge, H. Du, S. A. Fairhurst, R. C. Haddon, H. Oberhammer, S. Parsons, J. Passmore, M. J. Schriver, L. H. Sutcliffe, and N. P. C. Westwood, *J. Chem. Soc., Dalton Trans.*, **2000**, 3365.

9 a) T. Welton, *Chem. Rev.*, **99**, 2071 (1999). b) J. Dupont, R. F. de Souza, and P. A. Z. Suarez, *Chem. Rev.*, **102**, 3667 (2002).

10 Although some imidazolium-based RT ionic liquids containing anions with magnetic ions have been reported, their characterizations and magnetic studies are insufficient. [EMI][$Fe^{III}Cl_4$]: a) Y. Katayama, I. Konishiike, T. Miura, and T. Kishi, *J. Power Sources*, **109**, 327 (2002). [BMI][$Fe^{III}Cl_4$]: b) M. S. Sitze, E. R. Schreiter, E. V. Patterson, and R. G. Freeman, *Inorg. Chem.*, **40**, 2298 (2001). c) M. H. Valkenberg, C. deCastro, and W. F. Holderich, *Appl. Catal., A*, **219**, 372 (2001). d) F. Shi, J. Peng, and Y. Deng, *J. Catal.*, **219**, 372 (2003). e) W. Xu, E. I. Cooper, and C. A. Angell, *J. Phys. Chem. B*, **107**, 6170 (2003). f) S. Hayashi and H. Hamaguchi, *Chem. Lett.*, **33**, 1590 (2004). [BDMI][$Fe^{III}Cl_4$]: g) P. Kolle and R. Dronskowski, *Inorg. Chem.*, **43**, 2803 (2004). h) Q.-G. Zhang, J.-Z. Yang, X.-M. Lu, J.-S. Gui, and M. Huang, *Fluid Phase Equilib.*, **226**, 207 (2004).

11 a) G. Saito, "Ionic Liquids: The Front and Future of Material Development," ed by H. Ohno, CMC, Tokyo (2003), pp. 137–143. b) Y. Yoshida, J. Fujii, K. Muroi, A. Otsuka, G. Saito, M. Takahashi, and T. Yoko, *Synth. Met.*, **153**, 421 (2005).

12 S. P. Wicelinski, R. J. Gale, K. M. Pamidimukkala, and R. A. Laine, *Anal. Chem.*, **60**, 2228 (1988).

13 S. P. Wicelinski, R. J. Gale, S. D. Williams, and G. Mamantov, *Spectrochim. Acta, Part A*, **45**, 759 (1989).

14 J. S. Wilkes, J. A. Levisky, R. A. Wilson, and C. L. Hussey, *Inorg. Chem.*, **21**, 1263 (1982).

15 a) A. Noda, K. Hayamizu, and M. Watanabe, *J. Phys. Chem. B*, **105**, 4603 (2001). b) T. Nishida, Y. Tashiro, and M. Yamamoto, *J. Fluorine Chem.*, **120**, 135 (2003).

16 A. A. Fannin, D. A. Floreani, L. A. King, J. S. Landers, B. J. Piersma, D. J. Stech, R. L. Vaughn, J. S. Wilkes, and J. L. Williams, *J. Phys. Chem.*, **88**, 2614 (1984).

17 Y. Yoshida, A. Otsuka, and G. Saito, unpublished data.

18 P. B. Hitchcock, K. R. Seddon, and T. Welton, *J. Chem. Soc., Dalton Trans.*, **1993**, 2639.

19 a) G. A. Gamlen and D. O. Jordan, *J. Chem. Soc.*, **1953**, 1435. b) N. S. Gill, *J. Chem. Soc.*, **1961**, 3512. c) B. D. Bird and P. Day, *J. Chem. Phys.*, **49**, 392 (1968). d) J. C. Deaton, M. S. Gebhard, and E. I. Solomon, *Inorg. Chem.*, **28**, 877 (1989).

20 a) A. P. Ginsberg and M. B. Robin, *Inorg. Chem.*, **2**, 817 (1963). b) M. T. Vala and P. J. McCarthy, *Spectrochim. Acta, Part A*, **26**, 2183 (1970).

21 a) C. Furlani, E. Cervone, and V. Valenti, *J. Inorg. Nucl. Chem.*, **25**, 159 (1963). b) N. K. Hamer, *Mol. Phys.*, **6**, 257 (1963). c) D. Forster and D. M. L. Goodgame, *J. Chem. Soc.*, **1965**, 454.

22 a) S. Tait and R. A. Osteryoung, *Inorg. Chem.*, **23**, 4352 (1984). b) K. M. Dieter, C. J. Dymek, N. E. Heimer, J. W. Rovang, and J. S. Wilkes, *J. Am. Chem. Soc.*, **110**, 2722 (1988).

23 Y. Yoshida, K. Muroi, A. Otsuka, G. Saito, M. Takahashi, and T. Yoko, *Inorg. Chem.*, **43**, 1458 (2004).

24 a) R. Hagiwara, T. Hirashige, T. Tsuda, and Y. Ito, *J. Fluorine Chem.*, **99**, 1 (1999). b) R. Hagiwara, T. Hirashige, T. Tsuda, and Y. Ito, *J. Electrochem. Soc.*, **149**, D1 (2002).

25 H. Every, A. G. Bishop, M. Forsyth, and D. R. MacFarlane, *Electrochim. Acta*, **45**, 1279 (2000).

26 P. Walden, *Z. Phys. Chem.*, **78**, 257 (1912).

27 R. Hagiwara, K. Matsumoto, Y. Nakamori, T. Tsuda, Y. Ito, H. Matsumoto, and K. Momota, *J. Electrochem. Soc.*, **150**, D195 (2003).

28 a) A. B. McEwen, H. L. Ngo, K. LeCompte, and J. L. Goldman, *J. Electrochem. Soc.*, **146**, 1687 (1999). b) P. Bonhôte, A.-P. Dias, M. Armand, N. Papageorgiou, K. Kalyanasundaram, and M. Grätzel, *Inorg. Chem.*, **35**, 1168 (1996). c) S. A. Bolkan and J. T. Yoke, *J. Chem. Eng. Data*, **31**, 194 (1986). d) Z.-B. Zhou, H. Matsumoto, and K. Tatsumi, *Chem. Lett.*, **33**, 680 (2004). e) Z.-B. Zhou, H. Matsumoto, and K. Tatsumi, *Chem.—Eur. J.*, **10**, 6581 (2004). f) K. Matsumoto, R. Hagiwara, and Y. Ito, *J. Fluorine Chem.*, **115**, 133 (2002). g) K. Matsumoto, R. Hagiwara, R. Yoshida, Y. Ito, Z. Mazej, P. Benkič, B. Žemva, O. Tamada, H. Yoshino, and S. Matsubara, *Dalton Trans.*, **2004**, 144.

29 a) P. Wasserscheid and W. Keim, *Angew. Chem., Int. Ed.*, **39**, 3772 (2000). b) H. Olivier-Bourbigou and L. Magna, *J. Mol. Catal. A: Chem.*, **182–183**, 419 (2002). c) T. Welton, *Coord. Chem. Rev.*, **248**, 2459 (2004).

30 a) P. Wang, S. M. Zakeeruddin, R. Humphry-Baker, and M. Grätzel, *Chem. Mater.*, **16**, 2694 (2004). b) P. Wang, S. M. Zakeeruddin, J.-E. Moser, R. Humphry-Baker, and M. Grätzel, *J. Am. Chem. Soc.*, **126**, 7164 (2004).

31 R. J. Deeth, B. N. Figgis, and M. I. Ogden, *Chem. Phys.*, **121**, 115 (1988).

32 C. E. Schäffer and C. K. Jørgensen, *J. Inorg. Nucl. Chem.*, **25**, 159 (1963).

33 H. Du, R. C. Haddon, I. Krossing, J. Passmore, J. M. Rawson, and M. J. Schriver, *Chem. Commun.*, **2002**, 1836.

34 a) R. J. H. Clark, R. S. Nyholm, and F. B. Taylor, *J. Chem. Soc.*, **1967**, 1802. b) C. D. Burbridge and D. M. L. Goodgame, *J. Chem. Soc.*, **1968**, 1074.

35 A. Bondi, *J. Phys. Chem.*, **68**, 441 (1964).